Title

Electrophysiological Determination of Submembrane Na+ Concentration in Cardiac Myocytes

Journal

Biophysical Journal, 111(6)

ISSN

0006-3495

Authors

Hegyi, Bence

Bányász, Tamás

Shannon, Thomas R

et al.

Publication Date

2016-09-01

DOI

10.1016/j.bpj.2016.08.008

Peer reviewed

Biophysical Journal
Article

Biophysical Society

Electrophysiological Determination of Submembrane Na^+ Concentration in Cardiac Myocytes

Bence Hegyi,[1] Tamás Bányász,[1,4] Thomas R. Shannon,[5] Ye Chen-Izu,[1,2,3] and Leighton T. Izu[1,*]
[1]Department of Pharmacology, [2]Department of Biomedical Engineering, and [3]Department of Internal Medicine, Division of Cardiology, University of California, Davis, Davis, California; [4]Department of Physiology, Faculty of Medicine, University of Debrecen, Debrecen, Hungary; and [5]Department of Molecular Physiology and Biophysics, Rush University School of Medicine, Chicago, Illinois

ABSTRACT In the heart, Na^+ is a key modulator of the action potential, Ca^{2+} homeostasis, energetics, and contractility. Because Na^+ currents and cotransport fluxes depend on the Na^+ concentration in the submembrane region, it is necessary to accurately estimate the submembrane Na^+ concentration ($[Na^+]_{sm}$). Current methods using Na^+-sensitive fluorescent indicators or Na^+ -sensitive electrodes cannot measure $[Na^+]_{sm}$. However, electrophysiology methods are ideal for measuring $[Na^+]_{sm}$. In this article, we develop patch-clamp protocols and experimental conditions to determine the upper bound of $[Na^+]_{sm}$ at the peak of action potential and its lower bound at the resting state. During the cardiac cycle, the value of $[Na^+]_{sm}$ is constrained within these bounds. We conducted experiments in rabbit ventricular myocytes at body temperature and found that 1) at a low pacing frequency of 0.5 Hz, the upper and lower bounds converge at 9 mM, constraining the $[Na^+]_{sm}$ value to ~9 mM; 2) at 2 Hz pacing frequency, $[Na^+]_{sm}$ is bounded between 9 mM at resting state and 11.5 mM; and 3) the cells can maintain $[Na^+]_{sm}$ to the above values, despite changes in the pipette Na^+ concentration, showing autoregulation of Na^+ in beating cardiomyocytes.

INTRODUCTION

In the heart, Na^+ is a key modulator of the action potential (AP), Ca^{2+} homeostasis, energetics, and contractility. Na^+ cotransport of Ca^{2+} via the Na^+-Ca^{2+} exchanger has a prominent role in regulating contractility by controlling the amount of Ca^{2+} that is stored in the sarcoplasmic reticulum (1). Na^+ currents and cotransport fluxes are dependent on the free submembrane Na^+ concentration, $[Na^+]_{sm}$, which might not be equal to the bulk Na^+ concentration (2–4). Na^+-sensitive fluorescent indicators have been used to measure the bulk Na^+ concentration, but because the fluorescence signal from the bulk cytoplasm vastly overwhelms that from the submembrane volume, Na^+-sensitive fluorescent indicators cannot measure $[Na^+]_{sm}$. Na^+-sensitive electrodes and electron-probe microanalysis can, in principle, measure the submembrane Na^+ concentration but there are large uncertainties in the spatial position of the sampled region (5). On the other hand, electrophysiological measurements based on whole-cell patch-clamp methods are ideal for measuring submembrane ionic concentrations, because the current is determined by the submembrane ionic milieu. In this article, we use whole-cell patch-clamp methods to estimate the submembrane Na^+ concentration. Our method establishes upper and lower bounds of $[Na^+]_{sm}$, and the actual submembrane Na^+ concentration during the AP is constrained to lie between these bounds.

MATERIALS AND METHODS

Theoretical underpinnings

Our method does not define a particular value of the submembrane Na^+ concentration $[Na^+]_{sm}$. Rather, our method constrains $[Na^+]_{sm}$ between an upper bound, $[Na^+]^{ub}_{sm}$, and a lower bound, $[Na^+]^{lb}_{sm}$, so $[Na^+]^{lb}_{sm} \le [Na^+]_{sm} \le [Na^+]^{ub}_{sm}$. The difference $[Na^+]^{ub}_{sm} - [Na^+]^{lb}_{sm}$ is the range of uncertainty of $[Na^+]_{sm}$. Careful choice of experimental conditions, which we describe below, reduces the range of uncertainty, thereby clamping down on the value of $[Na^+]_{sm}$ like the jaws of a pair of pincers. Indeed, we will show that at a low pacing frequency (0.5 Hz), the mean values of upper and lower bounds are statistically indistinguishable.

Determining the upper bound

The method for determining the upper bound $[Na^+]^{ub}_{sm}$ is based on the fact that it is thermodynamically impossible for the peak membrane voltage, V_{peak}, to exceed the Na^+ equilibrium potential, E_{Na}

$$V_{peak} \le E_{Na} = \frac{RT}{F} \ln \frac{[Na^+]_o}{[Na^+]_{sm}}, \quad (1)$$

Submitted December 7, 2015, and accepted for publication August 8, 2016.
*Correspondence: ltizu@ucdavis.edu
Editor: Mark Cannell.
http://dx.doi.org/10.1016/j.bpj.2016.08.008

where R is the universal gas constant, T is the temperature (K), F is the Faraday constant (96,485 C/mol), and $[Na^+]_o$ is the extracellular Na^+ concentration. This inequality defines $[Na^+]_{sm}^{ub}$:

$$[Na^+]_{sm} \le [Na^+]_{sm}^{ub} \triangleq [Na^+]_o \exp\left(-\frac{FV_{peak}}{RT}\right). \quad (2)$$

In other words, the true subsarcolemmal Na^+ concentration, $[Na^+]_{sm}$ at the peak of the AP, is never greater than $[Na^+]_{sm}^{ub}$. As V_{peak} increases, $[Na^+]_{sm}^{ub}$ decreases, which reduces the range of uncertainty. Therefore, our strategy is to optimize experimental conditions that maximize V_{peak}. The optimal conditions are described in the Results.

Effect of resting membrane potential on the upper-bound estimate

The resting membrane potential could affect the measured peak voltage. If the resting membrane potential is more positive than ≈ -80 mV, then the fraction of Na^+ channel available to open during depolarization is <1, so the maximum voltage attained in the brief period before repolarization begins will likely be less than the Na^+ Nernst potential. If V_{true} is the peak voltage that would be measured if all Na^+ channels were available to open then $V_{true} \ge V_{measured}$ and we have the fortunate situation that we are *overestimating* the upper bound of the intracellular Na^+ concentration

$$[Na^+]_{sm} \le [Na^+]_{sm}^{ub} \le [Na]^{ub,measured}. \quad (3)$$

In other words, the calculated upper bound of the Na^+ concentration is conservative; the actual $[Na^+]_{sm}$ is lower. In all conditions, we analyzed only those records where the resting membrane potential was within a few mV of -80 mV (see Fig. 1 *C*).

Effect of junction potential on the upper-bound estimate

The measured peak membrane potential, V_{peak}, is the sum of the junction potential, V_{jp}, and the true membrane potential, V_{true},

$$V_{peak} = V_{true} + V_{jp}. \quad (4)$$

Accordingly,

$$\begin{aligned}[Na^+]_{sm} &\le [Na^+]_o \exp\left(-\frac{FV_{true}}{RT}\right) \\ &= [Na^+]_o \exp\left(-\frac{FV_{peak}}{RT}\right)\exp\left(+\frac{FV_{jp}}{RT}\right). \quad (5) \\ &= [Na^+]_{sm}^{ub}\end{aligned}$$

Note that if the junction potential is negative, then the range of uncertainty is narrowed. Conversely, if the junction potential is positive, the range of uncertainty is broadened. In our experiments, the junction potential was measured and nulled, so V_{jp} is set to 0 in Eq. 4, and therefore, the upper bound in Eq. 5 reduces to Eq. 2.

Determining the lower bound

The experiments to determine the lower bound will be described in detail later. Here, we explain the outline of the protocol and what the results mean. Briefly, the myocyte is held at -80 mV, then stepped to various positive potentials and the currents, $I(V)$, are measured. Subsequently, tetrodotoxin (TTX) is applied, the voltage-clamp protocol is repeated, and currents $I_{TTX}(V)$ are measured. Let V_{zero} be the clamp voltage when $I_{TTX}(V_{zero}) - I(V_{zero}) = 0$, which means that V_{zero} must equal E_{Na}. $[Na^+]_{sm}$ is then calculated from E_{Na}. We claim that this $[Na^+]_{sm}$ equals the submembrane concentration at rest. Before the application of the positive clamp voltage, the myocyte is held at -80 mV, the resting potential (see Fig. 5 *A*), for either 0.5 s or 2.0 s (depending on the experiment). Assuming a diffusion coefficient for NaCl of 0.1 μm^2/ms (6) and a diffusion length of 1 μm (half the length of a sarcomere) then the diffusion timescale is 10 ms. Thus, 0.5 s or 2 s equals 50 or 200 time constants, so any transient increase of $[Na^+]_{sm}$ from voltage steps before V_{zero} would be dissipated. Furthermore, because the voltage steps just before V_{zero} would have been close to E_{Na}, the amount of Na^+ entering through TTX-sensitive channels would have been small. Therefore, $[Na^+]_{sm}$ calculated from V_{zero} equals the resting concentration of $[Na^+]_{sm}$. This resting concentration, $[Na^+]_{sm}^{lb}$, is the lower bound for $[Na^+]_{sm}$ during the AP, that is, when the myocyte is paced.

Experimental methods

All animal handling and laboratory procedures were in accordance with the approved protocols of the local Institutional Animal Care and Use Committee conforming to the *Guide for the Care and Use of Laboratory Animals* published by the U.S. National Institutes of Health (8th edition, 2011).

Cell isolation

Ventricular myocytes were isolated from adult New Zealand White rabbits (male, 3–4 months old, 2.5–3 kg) by a standard enzymatic technique using collagenase type II (Worthington Biochemical, Lakewood, NJ) and protease type XIV (Sigma-Aldrich, St. Louis, MO) (7).

Electrophysiological recording of APs

Cells were transferred to a temperature-controlled plexiglass chamber (Cell Microsystems, Research Triangle Park, NC) and continuously superfused with a bicarbonate-containing Tyrode (BTY) solution with the composition (in mmol/L) 125 NaCl, 25 $NaHCO_3$, KCl 4, 1.2 $CaCl_2$, 1 $MgCl_2$, 10 HEPES, and 10 glucose, pH 7.4. Electrodes were fabricated from borosilicate glass (World Precision Instruments, Sarasota, FL) with tip resistances of 2–2.5 MΩ when filled with internal solution containing (in mmol/L) 100 K-Aspartate, 25 KCl, 10 NaCl, 3 Mg-ATP, 10 HEPES, 0.002 cAMP, 10 phosphocreatine dipotassium salt, and 0.01 EGTA, pH 7.3. It is important to note that this composition preserved the physiological Ca^{2+} cycling (8). In the experiments where $[Na^+]_i$ was changed, KCl concentration was adjusted to maintain $[Cl^-]_i$ and osmolarity. To study the impact of reduced $[Na^+]_o$ on the AP peak, NaCl was replaced by the appropriate amount of *N*-methyl-D-glucamine in BTY solution to restore its osmolarity; elevation of $[Na^+]_o$ was done simply by increasing the NaCl content of the BTY solution. To minimize the compensatory effect of changes in $[Na^+]_i$, each solution was applied for only 2 min, which was enough to reach a steady-state effect on V_{peak}. In current-clamp mode, cells were stimulated with suprathreshold depolarizing pulses (2 ms duration) delivered via the patch pipette. The series resistance was typically 3–5 MΩ and it was compensated by at least 85%. The seal condition was monitored during experiments, and cells were discarded if the series resistance increased by 10% during the experiment. Since access resistance might change during electrophysiological experiments, it is necessary to adjust the series resistance compensation. To assess its effect on the measured V_{peak}, we recorded APs after different degrees (0–10 MΩ) of series resistance compensations and demonstrated that they had no significant effect on the V_{peak} of the AP (for more details, see Fig. S1 in the Supporting Material).

Reported voltages are already corrected for the junction potential, which was 6 ± 0.5 mV. Axoclamp-2B and Axopatch 200B amplifiers (Axon Instruments, Union City, CA) were used for AP and I_{Na} measurements, respectively, and the signals were digitized by a Digidata 1440A A/D converter (Molecular Devices, Sunnyvale, CA).

Experiments were conducted at 36 ± 0.1°C.

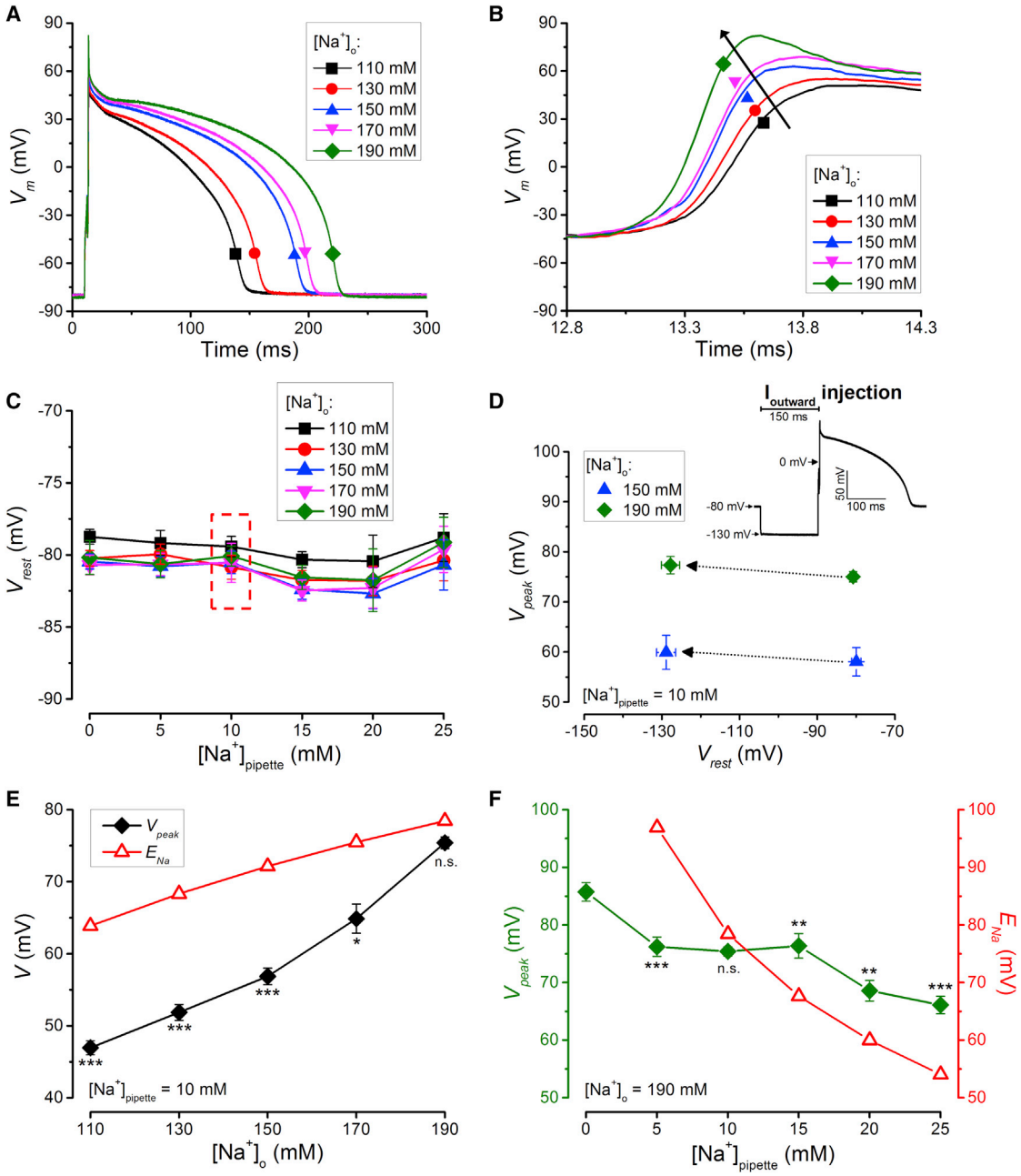

FIGURE 1 Optimizing conditions to estimate the $[Na^+]_{sm}$ upper bound. (*A*) Representative steady state APs from rabbit ventricular myocytes recorded with various $[Na^+]_o$. The pipette solution contained 10 mM Na^+ and the cells were paced at 2 Hz. (*B*) The AP upstroke after the stimulus transient shown on an expanded timescale. Both peak voltage (V_{peak}) and rate of rise increase with increasing $[Na^+]_o$. (*C*) The resting membrane potentials are largely the same across a broad range of $[Na^+]_o$ and $[Na^+]_{pipette}$ (n = 6–18 cells from three to seven animals). (*D*) V_{peak} is not increased further if a 150-ms-long hyperpolarization (to −130 mV) preceded the AP-eliciting stimulus. $[Na^+]_o$ was 150 mM (*green diamond*, n = 5 cells from three animals) or 190 mM (*blue triangle*, n = 7 cells from three animals). (*E*) V_{peak} (*black diamonds*) is approaching the predicted Nernst potential (*red triangles*) as $[Na^+]_o$ increases (n = 6–18 cells from three to six animals). Nernst potentials were calculated using 10 mM $[Na^+]_{pipette}$ as the intracellular $[Na^+]$. (*F*) Relation of the V_{peak} of the APs (*green diamonds*) to the Nernst potential of Na^+ (*red triangles*) obtained if intracellular $[Na^+]$ were the same as $[Na^+]_{pipette}$. $[Na^+]_o$ was fixed at 190 mM (n = 6–18 cells from three to seven animals). To see this figure in color, go online.

Measurement of the I_{Na} reversal potential in voltage-clamp mode

In voltage-clamped myocytes, I_{Na} was elicited by 10-ms-long depolarizing voltage steps from a holding potential of −80 mV at 2 Hz frequency. In experiments performed with 150 and 190 mM $[Na^+]_o$, the depolarizations ranged from +60 to +98 mV, whereas in those performed with 110 mM $[Na^+]_o$, they ranged from +50 mV to +88 mV (using 2 mV steps in both cases). (The reported voltages are already corrected for junction potentials.) To achieve good voltage control, series resistance was compensated by

95–99% in these experiments. The pipette solution contained 10 mM Na^+ in both cases (for ion composition of the external and internal solutions, see the previous section). Cells were pretreated with 10 μM nifedipine and 3 mM 4-aminopyridine to block L-type Ca^{2+} current and transient outward K^+ current, respectively. I_{Na} was measured as a current sensitive to 10 μM TTX ($I_{TTX} = I_{preTTX} - I_{postTTX}$) and the current amplitude was measured 2 ms after the beginning of the depolarizing voltage step. Reversal potential of Na^+ was calculated from the linear fitting of I_{Na}-V curves in each cell. The effect of TTX was completely reversible upon washout. Experiments were performed at 36 $\pm$ 0.1°C.

Statistical analysis

Data are expressed as the mean $\pm$ SE. The Kruskal-Wallis test (to compare multiple groups), Mann-Whitney U-test (to compare two groups), and paired or unpaired Student's t-test followed by analysis of variance were used where appropriate to determine statistical significance. Differences are deemed significant if $p < 0.05$*, $p < 0.01$**, or $p < 0.001$***.

RESULTS

Optimizing conditions for estimating the upper bound of $[Na^+]_{sm}$

First, we aimed to optimize the conditions for estimating the submembrane Na^+ concentration ($[Na^+]_{sm}$) in cardiac myocytes. Because the inward Na^+ current predominantly drives the upstroke of the AP, maximizing this current will push the peak voltage of the AP (V_{peak}) closer to the Nernst potential of Na^+ (E_{Na}) and therefore provide a tighter estimate of the upper bound of $[Na^+]_{sm}$, $[Na^+]_{sm}^{ub}$. Fig. 1 *A* shows representative APs recorded from rabbit ventricular myocytes paced at 2 Hz with various external Na^+ concentrations ($[Na^+]_o$) ranging from 110 mM to 190 mM, when the pipette solution contained 10 mM Na^+. Fig. 1 *B* shows the rising phase of the AP on an expanded timescale. Two notable features are evident in this graph. First, V_{peak} increases with increasing $[Na^+]_o$, and second, the rate of rise also increases with increasing $[Na^+]_o$. These qualitative changes reflect increased Na^+ current with higher $[Na^+]_o$ that increases the driving force. The larger the Na^+ current, the closer it drives V_{peak} toward E_{Na}. Therefore, it is desirable to use a higher $[Na^+]_o$ to measure V_{peak} to better estimate $[Na^+]_{sm}$. The highest $[Na^+]_o$ of 190 mM used in our experiment is constrained by the bath solution osmolarity required to maintain a stable seal. During the 2 min exposure to the 190 mM Na^+ solution, we saw no discernible change in myocyte morphology, and the access resistance remained constant. Before proceeding to use V_{peak} to estimate $[Na^+]_{sm}$, we conducted experiments to rigorously examine whether V_{peak} might be affected by potential complicating factors described below.

Testing the effect of resting membrane potential (V_{rest}) on V_{peak}

One potential complicating factor is the resting membrane potential (V_{rest}) that influences the availability of Na^+ channels to open during the upstroke of the AP. Fig. 1 *C* shows V_{rest} measured with various concentrations of Na^+ in the bath ($[Na^+]_o$) and in the pipette ($[Na^+]_{pipette}$). There is no statistically significant difference in V_{rest} between the groups with $[Na^+]_o$ in theh range 130–190 mM (Kruskal-Wallis test, $p = 0.08$). V_{rest} of the $[Na^+]_o$ 110 mM group showed a slight depolarization of ~3 mV, which was statistically significantly different from the 130 mM group (Mann-Whitney U-test, $p = 0.02$). However, given the flatness of the Na^+ inactivation, h, gating variable around −80 mV, it is unlikely that this slight depolarization in the $[Na^+]_o = 110$ mM group is the cause of the slowed rate of rise of the AP. The above data show that V_{rest} is about −80 mV across a broad range of $[Na^+]_o$ and most of the Na^+ channels should be available for activation.

We further examined Na^+ channel availability by hyperpolarizing the membrane for 150 ms before the AP was elicited, as shown in Fig. 1 *D*. An outward current of 3 nA was injected into the cell through the patch pipette to hyperpolarize the membrane potential to −130 mV, which should maximize the Na^+ channel availability. When APs were evoked from this voltage, there was no statistically significant change in V_{peak} in the $[Na^+]_o = 150$ mM or $[Na^+]_o =$ 190 mM groups.

To get a measure of how far our conditions are from optimal, we compared the measured V_{peak} at different $[Na^+]_o$ to the predicted value of E_{Na} assuming that $[Na^+]_{sm}$ equals the pipette Na^+ concentration ($[Na^+]_{pipette}$) of 10 mM. We used the value of 10 mM for two reasons, first simply because it was a round number close to the value of the bulk Na^+ concentration of 8 mM determined by Despa et al. (9), who used the same species, pacing rate, and temperature as we did, and second because, as experiments described in the next sections show, $[Na^+]_{sm}$ is constrained between 9 and 11.5 mM. Please note that we are not assuming that 10 mM is the actual value of $[Na^+]_{sm}$; it is used only to roughly estimate the position from an unknown, but reasonably constrained, ideal. Fig. 1 *E* shows the approach of V_{peak} to the putative E_{Na}. The difference between V_{peak} and E_{Na} diminishes monotonically as $[Na^+]_o$ increases. When $[Na^+]_o$ is 190 mM, V_{peak} is 75.41 $\pm$ 0.81 mV ($n = 18$), which is ~4 mV below the predicted $E_{Na} = 79$ mV. Hence, using the $[Na^+]_o = 190$ mM condition to measure the V_{peak} gives a close estimate of E_{Na}, which gives an optimal condition for estimating the upper bound of $[Na^+]_{sm}$.

The effect of changing $[Na^+]_{pipette}$ on V_{peak}

Next, we examined how changing the $[Na^+]_{pipette}$ would influence the V_{peak}. Fig. 1 *F* shows V_{peak} changes with different $[Na^+]_{pipette}$ values, whereas $[Na^+]_o$ was fixed at 190 mM. The overall trend shows that V_{peak} was higher at lower $[Na^+]_{pipette}$ values as E_{Na} increases. However, in comparing to the E_{Na} calculated under the assumption

$[Na^+]_i = [Na^+]_{pipette}$, V_{peak} was far below the calculated E_{Na} for $[Na^+]_{pipette} \leq 5$ mM and far above the calculated E_{Na} for $[Na^+]_{pipette} \geq 15$ mM. These data suggest that the actual intracellular $[Na^+]$ could differ from what is applied in the pipette when the cell was paced under physiological conditions (undergoing excitation-contraction at body temperature, which differs from the conventional voltage-clamp condition). Interestingly, the V_{peak} was maintained at ~75 mV for $[Na^+]_{pipette}$ values ranging from 5 to 15 mM, indicating autoregulation of the intracellular Na^+ concentration in this range (see the section on autoregulation, below).

Testing whether other ion channels might affect V_{peak}

The difference between V_{peak} and E_{Na} is minimized when the Na^+ current greatly dominates all other currents. We therefore examined the effect of transient outward current (I_{to}) and L-type Ca^{2+} current ($I_{Ca\text{-}L}$) on V_{peak}. The rapidly activating K^+ current, I_{to}, is likely to be the major contaminating current. We measured APs in the presence of the I_{to} blocker 4-aminopyridine (3 mM) when $[Na^+]_o$ was 190 mM (see Fig. 2 *A*); there was no significant difference in V_{peak} (77.16 ± 1.07 mV vs. 77.82 ± 0.50 mV in control and in 4-aminopyridine, respectively, $n = 6$, $p = 0.45$), indicating that I_{to} was not yet activated when the AP reached its peak, although during phase 1 repolarization, the role of I_{to} is obvious. To assess the effect of $I_{Ca\text{-}L}$ on V_{peak}, we measured APs in the presence of the $I_{Ca\text{-}L}$ blocker nifedipine (10 μM) when $[Na^+]_o$ was 190 mM. Again, blocking $I_{Ca\text{-}L}$ yielded no significant difference in V_{peak}, although it caused a decrease in the AP plateau and duration ($n = 6$, data not shown).

We further investigated how V_{peak} might be affected by Na^+-channel modulation. We modified the Na^+ channel opening time using anemone toxin (ATX-II), which inhibits the inactivation of voltage-gated Na^+ channels. Application of 5 nM ATX-II significantly increased AP duration and elevated the AP plateau, but it had no discernible effect on V_{peak} and the maximal rate of rise (Fig. 2 *B*). Indeed, the V_{peak} is determined by the fast Na^+ current, as evidenced by the fact that partial blockade of the Na^+ channel pore by 1 μM TTX ($\approx IC_{50}$) significantly decreased the V_{peak}, the maximal rate of rise, and the AP plateau (Fig. 2 *C*).

The fact that the V_{peak} is within 4 mV of the predicted E_{Na} when $[Na^+]_o = 190$ mM means that under this condition, I_{Na} dominantly determines V_{peak} at the moment of the AP peak when the contribution from other currents is negligible.

$[Na^+]_{sm}$ and the range of autoregulation

Because the value of V_{peak} can approach but not exceed E_{Na}, the Na^+ concentration calculated from the V_{peak} (using Eq. 2) gives the upper bound of $[Na^+]_{sm}$ (see Materials and Methods for theoretical underpinnings). Fig. 3 *A* shows the upper bounds of $[Na^+]_{sm}$ calculated from the V_{peak}

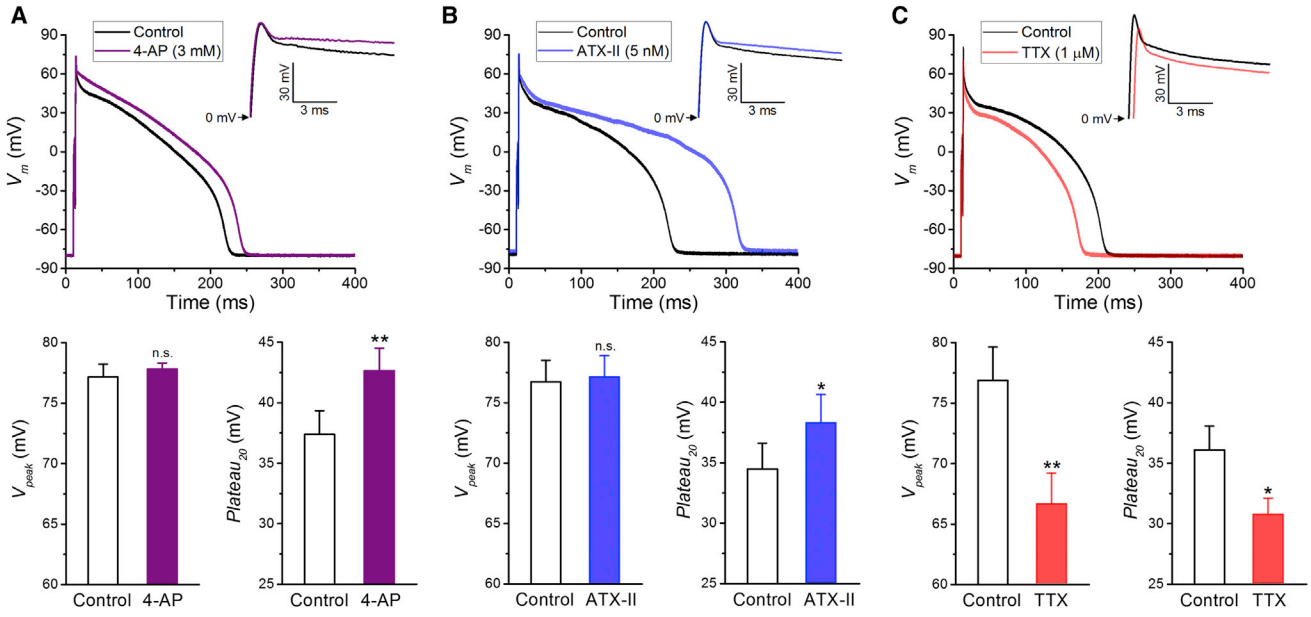

FIGURE 2 V_{peak} is predominantly set by the Na^+ influx, and is insensitive to I_{to}. (*A*) Representative APs in control (*black*) and after 4-aminopyridine treatment (*purple*) at 2 Hz steady-state pacing. 4-aminopyridine increased the AP duration and plateau voltages (already during phase 1 repolarization), but it had no effect on V_{peak} ($n = 6$ cells from three animals). $[Na^+]_o$ and $[Na^+]_{pipette}$ were 190 mM and 5 mM, respectively. (*B* and *C*) Representative APs recorded in control (*black*) and after ATX-II (*B*, *blue*) or TTX (*C*, *red*) pretreatment. Cells were continuously paced at 2 Hz. $[Na^+]_o$ of 190 mM and $[Na^+]_{pipette}$ of 10 mM were used. Inhibition of I_{Na} inactivation by ATX-II had no effect on V_{peak} (*B*), whereas partial blockade of the Na^+ channel pore by TTX significantly decreased the peak voltage (*C*). Plateau voltages were increased by ATX-II and decreased by TTX ($n = 5$ cells from two animals and 4 cells from two animals in ATX-II and TTX, respectively). To see this figure in color, go online.

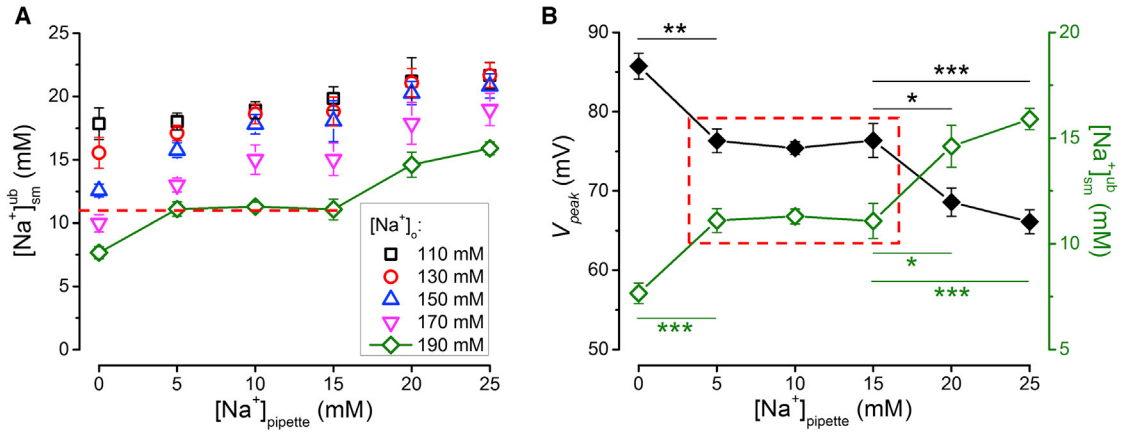

FIGURE 3 Autoregulation of $[Na^+]_{sm}$. (*A*) The calculated upper bounds of $[Na^+]_{sm}$ obtained with various $[Na^+]_o$. For $[Na^+]_{pipette}$ between 5 and 15 mM, no significant difference can be found in the upper bound of $[Na^+]_{sm}$, whose level is indicated by a dashed red line and referred to as a range of autoregulation. The cells were paced at 2 Hz. (*B*) The measured peak AP voltages (*black diamonds*) recorded with various $[Na^+]_{pipette}$ and fixed $[Na^+]_o$ at 190 mM are shown with the corresponding $[Na^+]_{sm}$ upper bounds (*green open symbols*) (n = 6–18 cells from three to seven animals). To see this figure in color, go online.

obtained with various internal and external Na^+ concentrations. The values obtained with $[Na^+]_o$ = 190 mM gives the *least* upper bound of $[Na^+]_{sm}$.

Interestingly, for $[Na^+]_{pipette}$ values ranging between 5 and 15 mM, there are no significant differences in measured V_{peak} (evaluated by analysis of variance at a significance level of 0.05), as shown in Fig. 3 *B* (*red box*), indicating an autoregulation of $[Na^+]_{sm}$. Outside of this range, V_{peak} changes significantly (Fig. 3 *B*). However, the change in V_{peak} is still less than the value predicted assuming no autoregulation (see Fig. 1 *F*), indicating that the cell can still regulate $[Na^+]_{sm}$ to some degree even at these extreme pipette Na^+ concentrations. Within the autoregulation range, the measured V_{peak} gives an upper bound of 11 mM for $[Na^+]_{sm}$ (Fig. 3 *B*, *red box*). Hence, our data reveal that the cell has the ability to autoregulate $[Na^+]_{sm}$ to ~11 mM when $[Na^+]_{pipette}$ is in the range 5–15 mM. (This also justifies the use of 10 mM $[Na^+]_{pipette}$ in Fig. 1, *E* and *F*).

Frequency dependence of $[Na^+]_{sm}$

Previous studies using fluorescent Na^+ indicators show that the average intracellular Na^+ concentration decreases at lower pacing frequency (9,10). We investigated the effect of pacing frequency on $[Na^+]_{sm}$. As shown in Fig. 4 *A*, V_{peak} increased by ~6 mV when the pacing frequency was reduced to 0.5 Hz from the previously applied 2 Hz. Accordingly, the upper bound of $[Na^+]_{sm}$ decreased from 11.68 ± 0.71 mM at 2 Hz to 9.46 ± 0.72 mM at 0.5 Hz (Fig. 4 *A*).

The lower V_{peak} at 2 Hz might be partially attributable to incomplete activation of the Na^+ channel. To test this, we modified V_{rest} to maximize Na^+ channel availability by injecting hyperpolarizing current for 150 ms before the AP

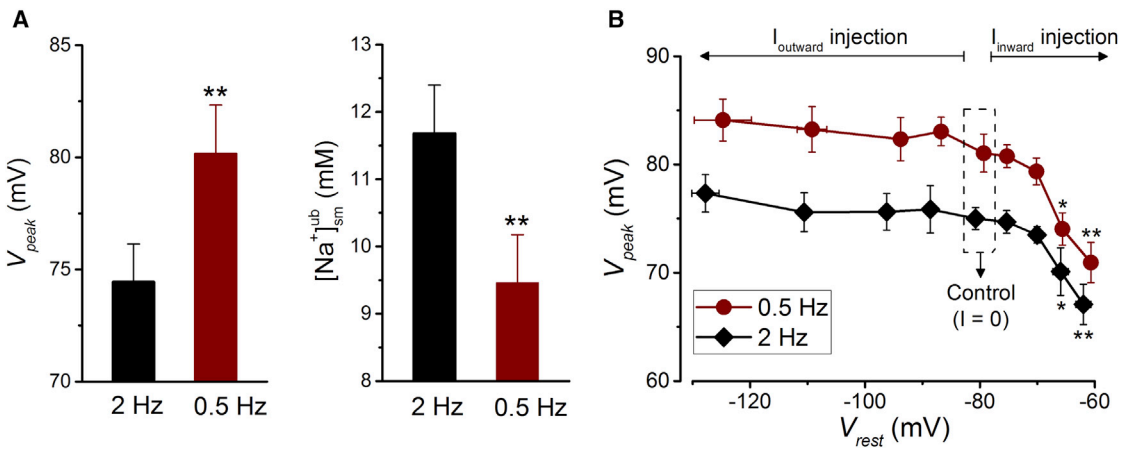

FIGURE 4 Frequency response of $[Na^+]_{sm}$. (*A*) Frequency dependence of V_{peak} and the calculated upper bound of $[Na^+]_{sm}$ (n = 6 cells from three animals). These self-controlled experiments were performed in 190 mM $[Na^+]_o$ and 10 mM $[Na^+]_{pipette}$. (*B*) The frequency-dependent difference in the AP peak was maintained even if the membrane potential was hyperpolarized or slightly depolarized by a current injection for 150 ms before the AP upstroke (n = 7 cells from three animals). To see this figure in color, go online.

upstroke (Fig. 4 *B*). The data show that the V_{peak} values are largely maintained during injection of the hyperpolarizing outward current, indicating no further increase of channel availability from $V_{rest} = -80$ mV to -130 mV. Therefore, the increased V_{peak} at 0.5 Hz vs. 2 Hz reports the true difference in $[Na^+]_{sm}$ that decreases at the lower pacing frequency.

The data in Fig. 4 *B* also show that injecting an inward current to depolarize the cell reduced Na^+-channel availability and decreased V_{peak}. This is undesirable, because decreasing V_{peak} increases the upper bound, thereby broadening the range of uncertainty of $[Na^+]_{sm}$.

Measurement of $[Na^+]_{sm}$ in the resting myocyte using the I_{Na} reversal potential

To estimate the resting $[Na^+]_{sm}$, we used a voltage-clamp protocol to determine the potential at which I_{Na} reverses (see Determining the Lower Bound in Materials and Methods for more information about why this method gives the resting $[Na^+]_{sm}$). The rapidly activating phase of I_{Na} largely overlaps with the capacitive transient, making it almost impossible to accurately measure the peak of I_{Na}. However, by minimizing the capacitive transient, the decaying phase of I_{Na} can be discerned and used to find the reversal potential of I_{Na}.

We took the following approach to accurately measure the reversal potential of I_{Na}. First, we carefully compensated the membrane capacitance and series resistance to 95–99% to minimize the capacitive transient. Second, we ensured that I_{Na} was the dominant current by minimizing other rapidly activating currents. We used 3 mM 4-aminopyridine and 10 μM nifedipine to inhibit I_{to} and $I_{Ca\text{-}L}$, respectively. Third, to further test whether I_{Na} dominates the measured current, we applied 10 μM TTX (which is very selective at this concentration and almost completely blocks the voltage-gated Na^+ channels) to isolate I_{Na} (Fig. 5 *A*). Representative TTX-sensitive current traces, evoked by short

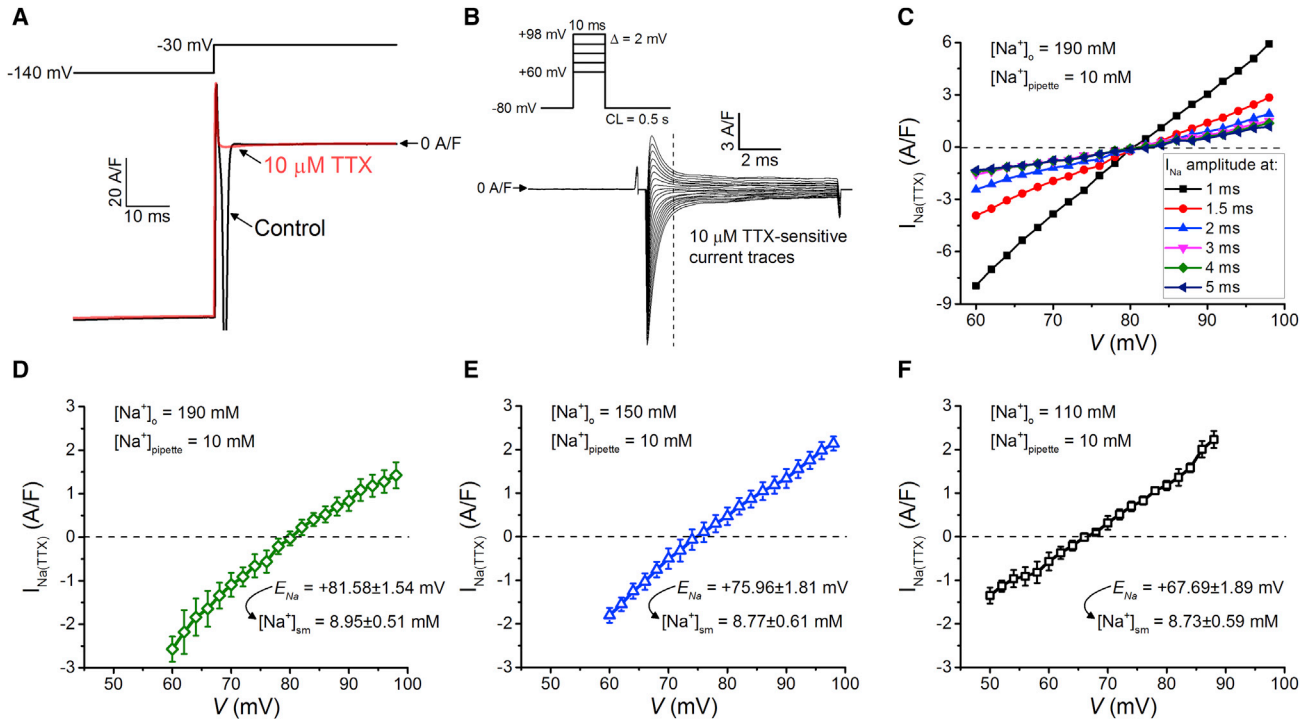

FIGURE 5 Using the reversal potential of I_{Na} to measure the $[Na^+]_{sm}$ lower bound. (*A*) Representative current traces evoked by depolarizations to -30 mV from a -140 mV holding potential in control and after application of 10 μM TTX. Cells were pretreated with 10 μM nifedipine and 3 mM 4-aminopyridine to avoid contamination with $I_{Ca\text{-}L}$ and I_{to}. The I_{Na} peak was out of the measuring range (>10 nA) in control, but it was almost completely blocked by TTX. (*B*) Representative TTX-sensitive current traces evoked by short (10 ms) depolarizing steps from a -80 mV holding potential delivered at 2 Hz frequency (see the voltage protocol in the inset). The vertical dashed line represents the time point where the currents were measured (2 ms from the beginning of the depolarization); at earlier time points, the current can overlap with the capacitive transient. (*C*) There was no difference in the E_{Na} value when *I-V* plots were made by measuring TTX-sensitive I_{Na} amplitude at different time points of the depolarization pulses (except at <1 ms, where the current almost completely overlaps with the capacitive transient). To avoid possible contamination with the capacitive transient, we measured the current 2 ms after the beginning of the depolarization, where its amplitude was still reasonably big (indicated by a vertical dashed line in (*B*)). (*D*) The current-voltage relationship of TTX-sensitive current measured in 190 mM $[Na^+]_o$ and 10 mM $[Na^+]_{pipette}$ ($n = 5$ cells from two animals). (*E*) E_{Na} was ~+76 mV, and the corresponding $[Na^+]_{sm}$ was ~8.8 mM in conditions close to the physiological (150 mM $[Na^+]_o$ and 10 mM $[Na^+]_{pipette}$) ($n = 6$ cells from three animals). (*F*) E_{Na} was significantly shifted to less positive potentials, but calculated $[Na^+]_{sm}$ was not changed when $[Na^+]_o$ was decreased to 110 mM ($n = 4$ cells from two animals). In these experiments, TTX-sensitive current was evoked between +50 mV and +88 mV to resolve better the range of interest. To see this figure in color, go online.

depolarizing voltage pulses between +60 and +98 mV, are shown in Fig. 5 *B*. The reversal potential of I_{Na} was obtained from the *I-V* plots (Fig. 5 *C*). The data show that there is no difference in the reversal potential of I_{Na} when *I-V* plots were made by taking TTX-sensitive I_{Na} amplitude at different time points of the depolarization pulse away from the capacitive transient, demonstrating the consistency of such measurement. We measured I_{Na} 2 ms after the onset of voltage pulse where the current amplitude was reasonably big (Fig. 5 *B*, *vertical dashed line*) for accurate determination of the reversal potential.

Using this method we measured the amplitude of I_{Na} at different voltage steps in cells exposed to 110 mM, 150 mM, and 190 mM $[Na^+]_o$, as shown in Fig. 5, *D–F*. The reversal potential of I_{Na} was obtained by a linear fitting of the *I-V* plot for each cell ($R^2 \geq 0.97$ in all cases). We calculate $[Na^+]_{sm}$ in each cell using Eq. 1. The mean $[Na^+]_{sm}$ values were 8.95 ± 0.51 mM, 8.77 ± 0.61, and 8.73 ± 0.59 for $[Na^+]_o$ of 190, 150, and 110 mM, respectively (see Fig. 5, *D–F*). There is no statistically significant difference between these groups, showing that the $[Na^+]_{sm}$ value is ~9 mM when $[Na^+]_o$ is in the range 110–190 mM.

The value of $[Na^+]_{sm}$ determined from measurements using this voltage-clamp protocol reports the value of $[Na^+]_{sm}$ in the resting myocyte for three reasons: 1) the myocyte is at resting condition during most of the 500 ms cycle length, except during the 10 ms voltage pulse; 2) the depolarizing voltage pulses are in the vicinity of E_{Na}, so the Na^+ influx is small; and 3) during the brief 2 ms window when the reversal potential is determined, the total Na^+ entry from other transporters such as the sodium-calcium exchanger and Na^+-K pump would not significantly change the Na^+ concentration. Furthermore, the $[Na^+]_{sm}$ value measured in the resting myocyte sets the lower bound for the submembrane Na^+ concentration during diastole.

Importantly, our data show that the lower bound of $[Na^+]_{sm}$ using this voltage-clamp protocol (8.95 ± 0.51 mM) (Fig. 5 *D*) is statistically indistinguishable from the upper bound of $[Na^+]_{sm}$ measured at the peak of the AP in the myocyte paced at 0.5 Hz (9.15 ± 0.60 mM; *t*-test, $p = 0.57$) (Fig. 4 *B*). Given that the actual value of $[Na^+]_{sm}$ is constrained between the upper bound and the lower bound, the fact that these two bounds converge to ~9 mM leads to a logical deduction that the actual $[Na^+]_{sm}$ is this value.

DISCUSSION

Electrophysiological approach to measure submembrane Na^+ concentration

In this article, we developed a new, to our knowledge, method—perhaps the only method—for estimating the free submembrane Na^+ concentration, $[Na^+]_{sm}$. Our method constrains $[Na^+]_{sm}$ between an upper bound, $[Na^+]^{ub}_{sm}$, estimated at the peak of the AP and a lower bound, $[Na^+]^{lb}_{sm}$, measured at the resting state. $[Na^+]_{sm}$ is bounded by the inequalities $[Na^+]^{lb}_{sm} \leq [Na^+]_{sm} \leq [Na^+]^{ub}_{sm}$. Reducing the difference between the upper and lower bounds squeezes in the value of $[Na^+]_{sm}$. In fact, at a low pacing frequency of 0.5 Hz, the upper and lower bounds are statistically indistinguishable, leading to the conclusion that the actual $[Na^+]_{sm}$ is ~9 mM (see the last paragraph in Results). However, for this method to be rigorously correct and practical, we must address two questions. $[Na^+]^{ub}_{sm}$ is defined as the upper bound at the time the AP reaches its peak, t_{peak}. In other words, the true $[Na^+]_{sm}$ at t_{peak} is bounded above by $[Na^+]^{ub}_{sm}$. However, we are interested in knowing whether $[Na^+]^{ub}_{sm}$ is the maximum value throughout the AP and diastole and not only at t_{peak}. Therefore, the first question we must answer is whether $[Na^+]^{ub}_{sm}$ is larger than $[Na^+]_{sm}$ at all times. Because the concentration depends on the time integral of the Na^+ flux into and out of the submembrane compartment, $[Na^+]_{sm}$ could possibly be larger than at t_{peak}. We know of no experimental method to test this possibility, so we used the Shannon-Bers model (2) to calculate when $[Na^+]_{sm}$ takes its peak value and to compare that to the value at t_{peak}. Fig. S2 shows that calculated $[Na^+]_{sm}$ achieves its maximum value ~0.4 ms before t_{peak}, but the concentration is only 0.06 mM greater than $[Na^+]^{ub}_{sm}$, a difference of <1%, and the time when $[Na^+]^{ub}_{sm}$ is not the maximum is <1 ms. Thus, we can state with negligible error that $[Na^+]^{ub}_{sm}$ determined at t_{peak} is the upper bound throughout the AP and diastole.

To achieve a low upper bound and reduce the range of uncertainty of $[Na^+]_{sm}$, we maximize the Na^+ current by briefly (~2 min) exposing the myocytes to a high external Na^+ concentration of 190 mM, which is far above the physiological concentration of ~150 mM. The second question we must consider is whether this nonphysiological condition nullifies our method. To understand why the upper-bound estimate of $[Na^+]_{sm}$ obtained with $[Na^+]_o = 190$ mM is relevant to estimating $[Na^+]_{sm}$ under physiological conditions, we need to establish that the true submembrane Na^+ (i.e., not the upper bound) obtained with $[Na^+]_o = 190$ mM, $[Na^+]_{sm}(190)$, is greater than that obtained with $[Na^+]_o = 150$ mM. Because the driving force for Na^+ is greater with $[Na^+]_o = 190$ mM than with $[Na^+]_o = 150$ mM, the inequality seems intuitively true, but intuition is not necessarily a faithful guide because the total amount of Na^+ transported through the Na^+ channel also depends on the conductance and kinetics. This inequality cannot be tested experimentally with existing methods, so we tested it by simulation using the Shannon-Bers model (2) with $[Na^+]_o = 190$ or 150 mM and the pipette Na^+ concentration fixed to 10 mM. As shown in Fig. S3, the AP lengthens and the V_{peak}

increases slightly when $[Na^+]_o$ is 190 mM compared to 150 mM, similar to what is seen experimentally (Fig. 1 *A*). Importantly, $[Na^+]_{sm}$ is greater with $[Na^+]_o$ = 190 mM than with $[Na^+]_o$ = 150 mM (Fig. S3 *C*). We therefore have the inequalities

$$[Na^+]^{ub}_{sm}(150) \underset{(1)}{\geq} [Na^+]^{ub}_{sm}(190) \underset{(2)}{\geq} [Na^+]_{sm}(190) \underset{(3)}{\geq} [Na^+]_{sm}(150).$$

Inequality 1 simply follows from the fact that V_{peak} measured with $[Na^+]_o$ = 150 mM is less than that when $[Na^+]_o$ = 190 mM (Fig. 1 *A*) and from Eq. 2. Inequality 2 follows from Eq. 2. Inequality 3 is from the simulations. These inequalities are important because they tell us that under physiological conditions the true submembrane Na^+ concentration is still bounded from above by $[Na^+]^{ub}_{sm}(190)$. Practically, this means that exposing the cell briefly to 190 mM external Na^+ to obtain a large V_{peak} is a practical way of estimating the true submembrane Na^+ concentration when the external Na^+ is in the physiological range of 150 mM. Therefore, the submembrane Na^+ concentration satisfies the inequalities $[Na^+]^{lb}_{sm} \leq [Na^+]_{sm} \leq [Na^+]^{ub}_{sm}$. It is important to note that these inequalities hold throughout the AP.

Evaluation of the method

The method presented here is the first, to our knowledge, to directly measure the free submembrane Na^+ concentration; therefore, we cannot, by definition, validate the method. However, we can evaluate the method in terms of 1) consistency and 2) uncertainty. Because fluorescent indicator methods measure bulk Na^+ and a Na^+-selective electrode samples the local Na^+ at a position that is not well determined (5), whereas our method responds only to the submembrane environment, we cannot and do not expect the values reported to be equal. Nonetheless, consistency demands that our estimates be no lower than those reported by fluorescent indicator or Na^+-selective electrode. The Na^+ concentration depends on temperature (compare (10) and (9)), species (10–13), and pacing rate (5,9,12)). Despa et al. (9) used conditions similar to ours (rabbit ventricular cells, 36–37°C, similar pacing frequency), so their data set is the best to check for consistency of our method. At a pacing rate of 2 Hz, our method constrains $[Na^+]_{sm}$ to be between 9 mM and 11.5 mM. At a low pacing frequency of 0.5 Hz, the upper and lower bounds are statistically indistinguishable so we conclude that $[Na^+]_{sm}$ is ~9 mM. These values are larger than the 8.0 ± 1.1 mM (for pacing rates of 0.5 to 3 Hz) measured by Despa et al. (9) using a fluorescent indicator that predominantly reports the bulk Na^+ concentration. In resting (unstimulated) myocytes, Despa et al. found that the bulk Na^+ concentration was 6.6 ± 0.5 mM, whereas our value was larger at 9 mM. In both stimulated and unstimulated cells, our estimates are consistently no lower than Despa et al.'s, which is expected given the different environments the two methods are measuring.

There are two important corollaries that can be drawn from a comparison of Despa et al.'s results and ours. First, the difference between the submembrane and bulk compartments at rest, 9 mM vs. 6.6 mM, indicates a standing Na^+ gradient that needs to be maintained by membrane and diffusional fluxes. We will later estimate the time constant for exchange between the submembrane and bulk compartments. Second, pacing only modestly increases Na^+ in both the bulk and submembrane compartments. In the submembrane space, a change from 0.5 to 2.5 Hz increases $[Na^+]_{sm}$ no more than 28% (from 9 mM to ≤11.5 mM). In the bulk, the change is a similarly modest 23% (from 6.6 mM at rest to 8.1 mM for a change from 0.5 to 3 Hz).

Our estimate of $[Na^+]_{sm}$ ~ 10 mM is much lower than the submembrane (28 nm from the surface) Na^+ concentration value of ~40 mM by Wendt-Gallitelli et al., based on electron-probe microanalysis (EPMA). Because EPMA measures the total Na (free and bound), consistency demands that the estimate of Wendt-Gallitelli et al. be no lower than ours, which is clearly the case.

The method we present here is unlike other methods in that it does not produce a single number for the Na^+ concentration but rather constrains the value of $[Na^+]_{sm}$ to be in a range between an upper and lower bound, except in the singular case where the upper and lower bounds coincide. At any moment, there is a range of uncertainty of the actual value of $[Na^+]_{sm}$, and the magnitude of the range of uncertainty is $[Na^+]^{ub}_{sm} - [Na^+]^{lb}_{sm}$. As V_{peak} departs from E_{Na}, the magnitude of $[Na^+]^{ub}_{sm}$ increases, thereby increasing the range of uncertainty. Changes in V_{peak} could reflect true changes of $[Na^+]_{sm}$ or deviations from the ideal case where Na^+ current is the sole generator of the upstroke of the AP. Deviations can occur if Na^+ channel availability is low or if other currents, such as I_{to}, flow during the upstroke. We checked these possibilities by hyperpolarizing the cell before the stimulus (to maximize channel availability), modifying Na^+ channel gating with ATX-II, and using pharmacological blockers of possible contaminating currents. None of these manipulations altered V_{peak}, so we are confident that our recording conditions are likely to be near optimal and the range of uncertainty is about as narrow as can be expected. However, deviations from ideality may be more severe for higher

pacing frequencies, different species, or disease conditions. It must be borne in mind that uncertainty does not imply error; $[Na^+]_{sm}$ is still constrained to be between $[Na^+]_{sm}^{ub}$ and $[Na^+]_{sm}^{lb}$, even as the range becomes large.

Timescale for Na^+ exchange between submembrane and bulk compartments

A standing Na^+ gradient between the submembrane and bulk compartments is maintained by a balance between membrane transport fluxes and a diffusional flux between them. We can derive an order-of-magnitude estimate of the time constant for exchange between these compartments based on the differences in $[Na^+]_{sm}^{ub}$ at 0.5 and 2 Hz. If we assume that 1) most of the Na^+ entering the cell is via the Na^+ channel, 2) the amount entering the cell is independent of pacing frequency, and 3) most of the flux out of the submembrane space is due to diffusion, then we can get an analytic expression for steady-state $[Na^+]_{sm}$ (see the Supporting Material)

$$x_\infty(T) \equiv x(t = \infty; T) = \frac{A}{\gamma}(e^{\gamma\tau} - 1)\frac{1}{1 - e^{-\gamma T}}, \quad (6)$$

where A is the amplitude of the Na^+ flux, τ is the duration of the flux, T is the stimulation period, and γ is the rate constant for transfer between the submembrane compartment and the bulk. To eliminate the unknown A and τ, we form the difference ratio,

$$\Delta r \equiv \frac{x_\infty(T_2) - x_\infty(T_1)}{x_\infty(T_2)} = 1 - \frac{1 - e^{-\gamma T_2}}{1 - e^{-\gamma T_1}}. \quad (7)$$

In our experiments, $T_1 = 1/2$ and $T_2 = 2$. Using $x_\infty(T_2) = 9$ mM and $x_\infty(T_1) = 11.5$ mM, we get $\gamma = 3.02\ s^{-1}$ (see the Supporting Material). Although a number of simplifying assumptions were made to arrive at this transfer rate (discussed more fully in the Supporting Material), this value agrees well with the transfer rate constant of $2.482\ s^{-1}$ in the Shannon-Bers model (2). The corresponding time constant is $\tau = 1/\gamma = 330$ ms.

If the diffusion of NaCl between the submembrane and bulk compartments were the same as in water, then $D_{NaCl} \cong 1\ \mu m^2/ms$ (14,15); if it were the same as in the bulk cytoplasm, then $D \cong 0.1\ \mu m^2/ms$ (6). Assuming a diffusion length of $\ell = 1\ \mu m$, then the diffusion timescale is $\tau_D \sim \ell^2/D \sim 1 - 10$ ms. Even if tortuosity was halved, the diffusion coefficient, τ_D, would only double. The fact that $\tau \cong \tau_D$ suggests that either 1) diffusion in this submembrane or fuzzy space (4,16) is greatly slowed, perhaps by proteins or lipids that bind Na^+, or 2) membrane transport keeps replenishing the Na^+ lost to diffusion. These possibilities are not mutually exclusive.

Although our data point to a much slower decay of submembrane Na^+ than would be expected with free diffusion and no replenishment, our τ estimate is much shorter than the minutes timescale determined from EPMA (3). Because EPMA measures total Na (free and bound), perhaps the readiest explanation for the vast differences in timescales is that the longer timescale reflects the unbinding time of Na^+ from proteins or lipids in the submembrane space.

Na^+ autoregulation

When the cardiac myocyte is paced and undergoes excitation-contraction coupling, our data (Fig. 3) show that submembrane Na^+ concentration can be different from the pipette Na^+ concentration. This is in line with theoretical studies of Mathias et al. (17) and experimental studies by Ishizuka and Berlin (18) and Main et al. (19) but differs from the theoretical and experimental work of Mogul et al. (20). If the pipette could clamp the submembrane Na^+ concentration, then the slope of the curve in Fig. 3 *A* would be unity (as it is in Fig. 4 of (20)). Any departure from unit slope indicates an imbalance between flux from the pipette and other Na^+ fluxes across the cell membrane. However, our data show more than just an imbalance between these fluxes. The constant (flat) part of the curve in Fig. 3 *A* suggests an active *autoregulation* of $[Na^+]_{sm}$. Neither of the cited theoretical studies (17,20) or our modeling studies (see Fig. S4) reproduced the autoregulation of $[Na^+]_{sm}$. In our model simulation, $[Na^+]_{sm}$ rose linearly with pipette concentration, albeit with considerably less than unit slope, suggesting a certain degree of regulation. However, unlike in our experiments, the modeling results did not show constant $[Na^+]_{sm}$ despite changes in the pipette concentration from 5 to 15 mM. Such constancy suggests some feedback mechanism to maintain $[Na^+]_{sm}$ at a fixed point. The inadequacy of the models tells us that 1) the mathematical model description of the Na^+ fluxes in subcellular compartments may be incomplete, and 2) factors other than the submembrane Na^+ concentration may come into play to amplify (or attenuate) the Na^+ transport fluxes.

Effects of junction potential on our measurements

In voltage-clamp experiments, a liquid junction potential (JP) arises when two solutions are in contact that have different ionic compositions and motilities of those ions (21). The JP developing between pipette solution and bath is zeroed before seal formation as the standard procedure in patch-clamp technique. However, after seal formation when the membrane is ruptured, the pipette solution comes into contact with the cytosolic solution that is different from the bath solution, resulting in a different JP. This JP can be measured experimentally, and then numerically compensated during data analysis. In our experimental setting (using Ag/AgCl electrodes), the JP was measured to be 6 ± 0.5 mV. This value is less than the theoretically calculated

value of JP between 10 and 12 mV (with standard aspartate-based pipette solutions in normal Tyrode solution). As shown in Materials and Methods, the solutions we used in our experiments were different from that used in most previous publications. The most important difference is that our pipette solution contains no EGTA or other calcium buffer, and the bath solution is supplemented with 25 mM bicarbonate (therefore, the chloride concentration is lowered). The ionic composition of these solutions is much closer to the physiological environment of cardiac myocytes than the ionic milieu used in conventional biophysical experiments. Thus, we empirically measured JP and then subtracted the measured JPs in our data analysis.

Another technical problem may arise from the wide (110–190 mM) concentration range of Na^+ and Cl^- in the bath solution used in our experiments. The Ag/AgCl electrode is known to be sensitive to the Cl^- concentration of the medium (21), so we tested the JP at each Na^+ and Cl^- concentration. Our tests showed that the change in JP measured in different bath solutions was $< \pm 0.3$ mV. These changes were confirmed with the JP calculator function (22) of the Clampex program (Version 10, Molecular Devices).

Practical guide for electrophysiological determination of $[Na^+]_{sm}$

The following summarizes the steps we used to estimate $[Na^+]_{sm}$. Please note that the pipette solution uses a low EGTA concentration (0.01 mM) so normal Ca^{2+} cycling is preserved (8). High EGTA or BAPTA in the pipette increases the success rate of the experiments by eliminating myocyte contraction, but the resulting estimate of $[Na^+]_{sm}$ might not accurately reflect the actual physiological value, because the intracellular Ca^{2+} transient during the AP would be eliminated and the Na^+-Ca^{2+} exchanger would not function normally.

$[Na^+]_{sm}$ lower-bound measurement

Use the voltage-clamp protocol to measure the reversal potential of I_{Na} (as described in Fig. 5), which gives the Nernst potential of Na^+ in the resting myocyte; this is used to calculate the resting level $[Na^+]_{sm}$. The $[Na^+]_{sm}$ value at resting state sets the lower bound of $[Na^+]_{sm}$ during diastole and the entire cardiac cycle. This $[Na^+]_{sm}$ also provides a good value for setting the pipette Na^+ concentration in the following experiments.

$[Na^+]_{sm}$ upper-bound measurement

Use the current-clamp protocol to record the AP and measure V_{peak} using the following optimizing conditions (as described in Fig. 1): 1a) use $[Na^+]_o = 190$ mM and $[Na^+]_{pipette} = 10$ mM (for healthy rabbit ventricular myocytes); 1b) start from a resting potential of -80 mV or lower (if needed, a hyperpolarizing current can be used to yield $V_{rest} < -80$ mV); 1c) record the fast upstroke of the AP with high fidelity (the AP peak should be clearly separated from the stimulation pulse, with the R_a kept low, <4.5 MΩ). These optimizing conditions allow V_{peak} to approach the Nernst potential of Na^+. V_{peak} is used to estimate the $[Na^+]_{sm}$ upper bound according to Eq. 1.

$[Na^+]_{sm}$ autoregulation range

The autoregulation range reveals the cell's ability to maintain a constant Na^+ concentration despite perturbation from the pipette Na^+ concentration. This also means that as long as $[Na^+]_{pipette}$ is within the autoregulation range, the V_{peak} value is stable and provides a good measure of the $[Na^+]_{sm}$ upper bound.

Finally, the actual $[Na^+]_{sm}$ value during the cardiac cycle should be between the upper bound, measured at the peak of the AP, and the lower bound, measured at the resting state.

SUPPORTING MATERIAL

Supporting Materials and Methods and four figures are available at http://www.biophysj.org/biophysj/supplemental/S0006-3495(16)30668-3.

AUTHOR CONTRIBUTIONS

L.T.I., T.B., and Y.C.-I. conceived the project; L.T.I., T.B., and B.H. designed the research; B.H. did the experiments and analyzed the data; T.S. assisted in the initial modeling; and B.H., T.B., Y.C.-I., and L.T.I. wrote the article.

ACKNOWLEDGMENTS

We thank Zhong Jian and Rafael Shimkunas for their help in animal care and cell isolation.

Financial support was provided by National Institutes of Health (NIH) grants R01HL090880 to L.T.I. and Y.C.-I., R01HL105242 to L.T.I., R01HL123526 to Y.C.-I., American Heart Association (AHA) grant 14GRNT20510041 to Y.C.-I., and Hungarian Scientific Research Fund grant OTKA101196 to T.B.

REFERENCES

1. Despa, S., and D. M. Bers. 2013. Na^+ transport in the normal and failing heart—remember the balance. *J. Mol. Cell. Cardiol.* 61:2–10.
2. Shannon, T. R., F. Wang, …, D. M. Bers. 2004. A mathematical treatment of integrated Ca dynamics within the ventricular myocyte. *Biophys. J.* 87:3351–3371.
3. Wendt-Gallitelli, M. F., T. Voigt, and G. Isenberg. 1993. Microheterogeneity of subsarcolemmal sodium gradients. Electron probe microanalysis in guinea-pig ventricular myocytes. *J. Physiol.* 472:33–44.
4. Carmeliet, E. 1992. A fuzzy subsarcolemmal space for intracellular Na^+ in cardiac cells? *Cardiovasc. Res.* 26:433–442.
5. Cohen, C. J., H. A. Fozzard, and S. S. Sheu. 1982. Increase in intracellular sodium ion activity during stimulation in mammalian cardiac muscle. *Circ. Res.* 50:651–662.
6. Despa, S., J. Kockskämper, …, D. M. Bers. 2004. Na/K pump-induced $[Na]_i$ gradients in rat ventricular myocytes measured with two-photon microscopy. *Biophys. J.* 87:1360–1368.

7. Horvath, B., T. Banyasz, …, Y. Chen-Izu. 2013. Dynamics of the late Na^+ current during cardiac action potential and its contribution to afterdepolarizations. *J. Mol. Cell. Cardiol.* 64:59–68.
8. Banyasz, T., B. Horvath, …, Y. Chen-Izu. 2012. Profile of L-type Ca^{2+} current and Na^+/Ca^{2+} exchange current during cardiac action potential in ventricular myocytes. *Heart Rhythm.* 9:134–142.
9. Despa, S., M. A. Islam, …, D. M. Bers. 2002. Intracellular Na^+ concentration is elevated in heart failure but Na/K pump function is unchanged. *Circulation.* 105:2543–2548.
10. Despa, S., M. A. Islam, …, D. M. Bers. 2002. Intracellular [Na^+] and Na^+ pump rate in rat and rabbit ventricular myocytes. *J. Physiol.* 539:133–143.
11. Donoso, P., J. G. Mill, …, D. A. Eisner. 1992. Fluorescence measurements of cytoplasmic and mitochondrial sodium concentration in rat ventricular myocytes. *J. Physiol.* 448:493–509.
12. Harrison, S. M., E. McCall, and M. R. Boyett. 1992. The relationship between contraction and intracellular sodium in rat and guinea-pig ventricular myocytes. *J. Physiol.* 449:517–550.
13. Zaza, A., R. P. Kline, and M. R. Rosen. 1990. Effects of α-adrenergic stimulation on intracellular sodium activity and automaticity in canine Purkinje fibers. *Circ. Res.* 66:416–426.
14. Riquelme, R., I. Lira, …, R. Rodriguez-Vera. 2007. Interferometric measurement of a diffusion coefficient: comparison of two methods and uncertainty analysis. *J. Phys. D Appl. Phys.* 40:2769–2776.
15. Oliva, C., I. S. Cohen, and R. T. Mathias. 1988. Calculation of time constants for intracellular diffusion in whole cell patch clamp configuration. *Biophys. J.* 54:791–799.
16. Lederer, W. J., E. Niggli, and R. W. Hadley. 1990. Sodium-calcium exchange in excitable cells: fuzzy space. *Science.* 248:283.
17. Mathias, R. T., I. S. Cohen, and C. Oliva. 1990. Limitations of the whole cell patch clamp technique in the control of intracellular concentrations. *Biophys. J.* 58:759–770.
18. Ishizuka, N., and J. R. Berlin. 1993. β-Adrenergic stimulation does not regulate Na pump function in voltage-clamped ventricular myocytes of the rat heart. *Pflugers Arch.* 424:361–363.
19. Main, M. J., C. J. Grantham, and M. B. Cannell. 1997. Changes in subsarcolemmal sodium concentration measured by Na-Ca exchanger activity during Na-pump inhibition and β-adrenergic stimulation in guinea-pig ventricular myocytes. *Pflugers Arch.* 435:112–118.
20. Mogul, D. J., D. H. Singer, and R. E. Ten Eick. 1989. Ionic diffusion in voltage-clamped isolated cardiac myocytes. Implications for Na,K-pump studies. *Biophys. J.* 56:565–577.
21. Neher, E. 1992. Correction for liquid junction potentials in patch clamp experiments. *Methods Enzymol.* 207:123–131.
22. Barry, P. H. 1994. JPCalc, a software package for calculating liquid junction potential corrections in patch-clamp, intracellular, epithelial and bilayer measurements and for correcting junction potential measurements. *J. Neurosci. Methods.* 51:107–116.